

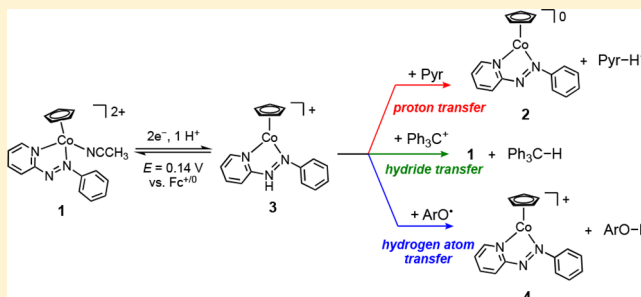
Protonation of a Cobalt Phenylazopyridine Complex at the Ligand Yields a Proton, Hydride, and Hydrogen Atom Transfer Reagent

Elizabeth A. McLoughlin,[†] Kate M. Waldie,[†] Srinivasan Ramakrishnan,[†] and Robert M. Waymouth^{*†}

Department of Chemistry, Stanford University, Stanford, California 94305, United States

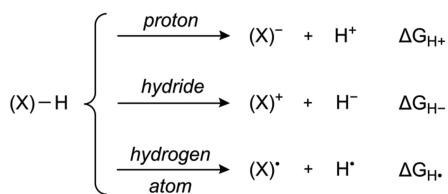
Supporting Information

ABSTRACT: Protonation of the Co(I) phenylazopyridine (azpy) complex [CpCo(azpy)] **2** occurs at the azo nitrogen of the 2-phenylazopyridine ligand to generate the cationic Co(I) complex [CpCo(azpyH)]⁺ **3** with no change in oxidation state at Co. The N–H bond of **3** exhibits diverse hydrogen transfer reactivity, as studies with a variety of organic acceptors demonstrate that **3** can act as a proton, hydrogen atom, and hydride donor. The thermodynamics of all three cleavage modes for the N–H bond (i.e., proton, hydride, and hydrogen atom) were examined both experimentally and computationally. The N–H bond of **3** exhibits a p*K*_a of 12.1, a hydricity of Δ*G*^o_{H–} = 89 kcal/mol, and a bond dissociation free energy (BDFE) of Δ*G*^o_{H•} = 68 kcal/mol in CD₃CN. Hydride transfer from **3** to the trityl cation (Δ*G*^o_{H–} = 99 kcal/mol) is exergonic but takes several hours to reach completion, indicating that **3** is a relatively poor hydride donor, both kinetically and thermodynamically. Hydrogen atom transfer from **3** to 2,6-di-*tert*-butyl-4-(4'-nitrophenyl)phenoxy radical (^tBu₂NPArO•, Δ*G*^o_{H•} = 77.8 kcal/mol) occurs rapidly, illustrating the competence of **3** as a hydrogen atom donor.



INTRODUCTION

Hydride, hydrogen atom, and proton transfers are key steps in many chemical and biological redox processes. These transformations can be mediated by organic molecules,^{1–3} transition metal hydrides,^{4–7} or proton and redox-active ligands bound to transition metal centers (Figure 1).^{8–18} A



(X) = Organic Molecule R, transition metal M, or M-(RAL)-H, where RAL = Redox-Active Ligand

Figure 1. Possible modes of hydrogen (H⁺, H[•], or H[–]) transfer.

detailed understanding of both the thermodynamics and kinetics of these hydrogen transfer processes^{2,4,19–25} are required in order to successfully exploit them for stoichiometric or catalytic redox reactions. Considerable effort has been devoted to understanding the hydrogen atom donor reactivity and X–H bond strengths of organic compounds^{1–3} and transition metal hydrides.^{4–6} More recently, the hydrogen atom donor reactivity of proton/redox-active ligands bound to transition metals have been shown to be strongly influenced

both by the nature of the transition metal and the ligand.^{8–18,26–32}

We recently described³³ the reversible two-electron reduction of the dicationic Co(III) complex [CpCo(azpy)(CH₃CN)] [ClO₄]₂ **1**, which bears the redox-active phenylazopyridine ligand (azpy).^{34–38} Herein, we show that protonation of the reduced neutral complex [CpCo(azpy)] **2** occurs at the azopyridine ligand to generate the cationic species [CpCo(azpyH)]⁺ **3**. Reactivity studies with appropriate organic acceptors demonstrate that **3** can act as a proton, hydrogen atom, and hydride donor (Figure 2). Spectroscopic, electrochemical, and computational characterization of **3** provide estimates of the heterolytic and homolytic dissociation free energies of the N–H bond in **3**.

RESULTS

Synthesis. The syntheses of [CpCo(azpy)(CH₃CN)] [ClO₄]₂ **1** [ClO₄]₂ and the two-electron reduced species [CpCo(azpy)] **2** were recently reported.^{33,39} Protonation of **2** with various strong acids including *N,N*-dimethylformaminium triflate ([DMFH][CF₃SO₃]) and trifluoromethanesulfonic acid (TfOH) occurs rapidly to generate the monocationic complex **3** (Figure 2). The protonated species **3** can be isolated in greater than 70% yield by precipitation of an acetonitrile solution into benzene followed by filtration.

Received: June 20, 2018

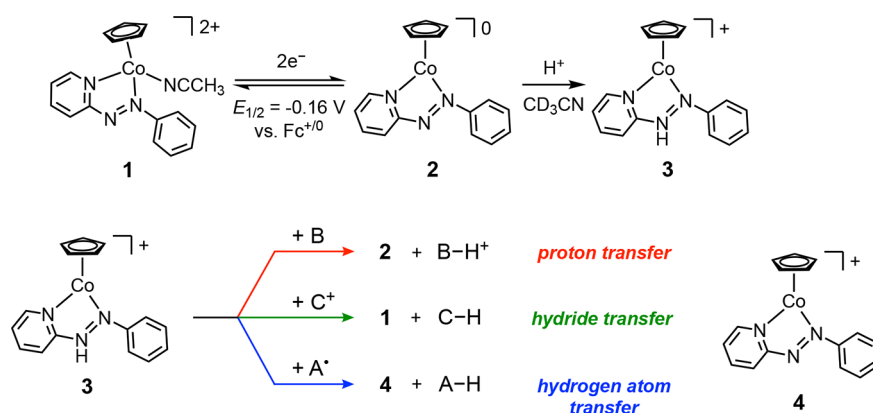


Figure 2. Generation of protonated complex 3, which acts as a proton, hydrogen atom, or hydride donor.

Solutions of complex 3 are stable in dried and degassed CD_3CN over the course of 24 h, as determined by ^1H NMR spectroscopy.

Characterization. Complex 3 is diamagnetic and displays clearly resolved resonances for the phenyl and pyridyl ring protons in the ^1H NMR spectrum. The cyclopentadienyl protons signal appears at 5.20 ppm, which is shifted downfield by 0.36 ppm compared to the neutral complex 2.³³ A similar downfield shift is seen for all aromatic signals, which is consistent with protonation to the monocationic complex. No upfield signal for a Co-hydride is observed by ^1H NMR, suggesting that the site of proton addition is not the metal, but rather the azopyridine ligand. Low temperature ^1H NMR studies in CD_3CN reveal a sharp singlet at 12.11 ppm at -37°C that integrates to one proton. As the temperature of the sample is increased to 23°C , this peak broadens and shifts upfield to 11.97 ppm (Figure S6). These observations suggest that protonation occurs at the azo nitrogen to form an N–H bond. The solid state infrared spectrum of 3 shows several broad absorbances from $2800\text{--}3200\text{ cm}^{-1}$ that are absent in the IR spectrum of 2 (Figure S7). These new high wavenumber features are consistent with the presence of an N–H group in 3 and further support that protonation occurs at the nitrogen of the azopyridine ligand.

Crystals of 3 suitable for X-ray diffraction were obtained by slow diffusion of diethyl ether into a saturated acetonitrile solution. The ORTEP structure of the complex modeled with the relevant hydrogen atom on the azopyridine nitrogen is shown in Figure 3. The proximity of the triflate counteranion to the azopyridine nitrogen likely suggests a hydrogen bonding interaction between the N–H bond and the triflate anion. Select bond lengths and angles for 3 are detailed in Table 1, along with the analogous parameters of the neutral species 2 for comparison.³³ The cobalt center of 3 has a two-legged piano stool geometry with the phenyl ring twisted out of the Co–azopyridine plane by 38° . Notably, the cobalt–nitrogen, nitrogen–carbon, and nitrogen–nitrogen bond lengths in the protonated complex 3 are almost identical (within 0.03 Å) to those of 2, indicating that the coordination environment at cobalt is relatively unperturbed upon protonation.

Density functional theory (DFT) was employed to provide further insights on the coordination geometry and electronic structure of these complexes (see Computational Details).³³ The corresponding bond lengths in the DFT-calculated structure of 3 are in excellent agreement with the experimentally determined values (Table 1). Coordination of

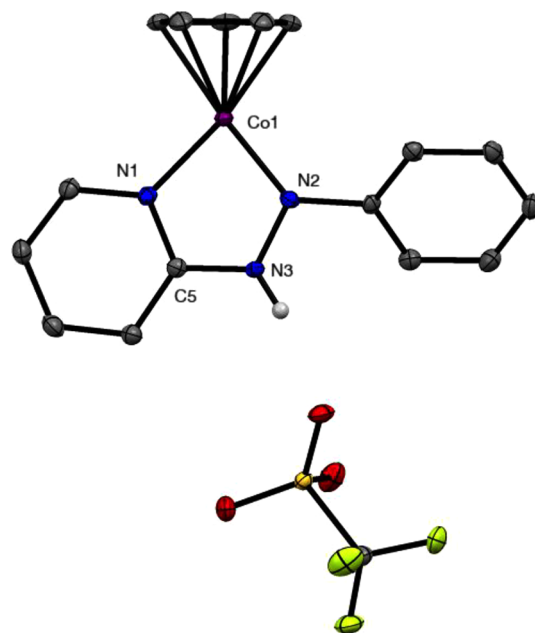


Figure 3. ORTEP structure of 3 with triflate counteranion, 50% probability ellipsoids. Hydrogen atoms are omitted for clarity except for the N–H atom.

Table 1. Experimental and Calculated Values for Selected Bond Lengths and Angles in 2 and 3

	2 ^a (exp.)	2 ^a (calc.)	3 (exp.)	3 (calc.)
Bond lengths (Å)				
Co–N1	1.869(2)	1.875	1.8962(14)	1.905
Co–N2	1.823(2)	1.838	1.8194(14)	1.812
Co–Cp ^b	2.06	2.08	2.07	2.07
N2–N3	1.348(3)	1.338	1.3618(19)	1.309
N2–C11	1.428(3)	1.429	1.429(2)	1.426
N3–C10	1.351(3)	1.363	1.358(2)	1.363
Bond angles (deg)				
N1–Co–N2	81.41(9)	81.56	83.33(6)	83.7

^aFrom ref 32. ^bAverage distance of bonds between Co and the Cp ring.

an acetonitrile ligand to make a six-coordinate complex is predicted to be unfavorable by ca. 19 kcal/mol. DFT analysis also predicts that the lowest energy structure of 3 is best formulated as low-spin Co(I). These results further support that protonation at the azopyridine ligand does not

significantly influence the bonding geometry or electronic structure at the Co center.

Electrochemistry. The electrochemical behavior of **1**, **2**, and **3** in acetonitrile was examined by cyclic voltammetry, as shown in Figure 4. As previously reported,³³ the voltammo-

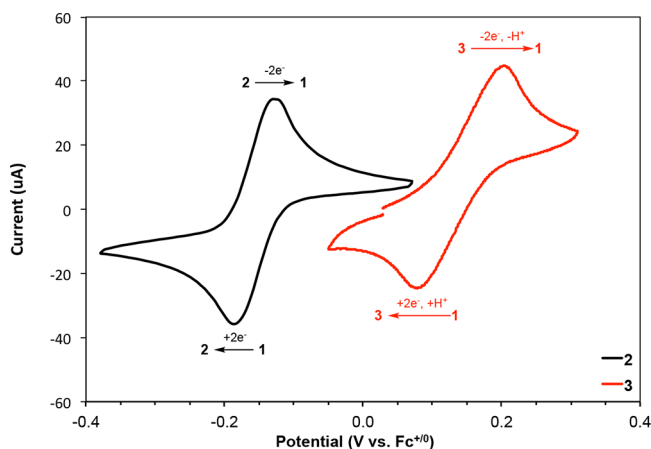
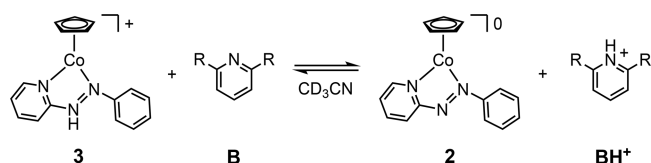


Figure 4. Cyclic voltammograms of **2** (1 mM Co, black trace) and **3** (1 mM Co, 13 mM [DMFH][OTf]/lutidine buffer, red trace) in acetonitrile with 0.1 M Bu₄NClO₄. Scan rate 100 mV/s.

gram of **2** in acetonitrile displays a reversible two electron oxidation at -0.16 V versus the ferrocenium/ferrocene couple ($\text{Fc}^{+/0}$). The voltammogram of **3** in the presence of a [DMFH][CF₃SO₃]/lutidine buffered acetonitrile solution displays a quasireversible oxidation at 0.14 V versus $\text{Fc}^{+/0}$, which has been identified as a two-electron process via controlled-potential electrolysis (Figure S5). In buffer, the oxidation wave can be assigned to the two-electron, one-proton oxidation of **3** to **1**, and the reduction wave to the two-electron, one-proton reduction of **1**.^{20,39} This assignment is corroborated by cyclic voltammetry studies of **3** in the absence of buffer (Figure S3, Supporting Information); in the absence of buffer, the voltammogram of **3** exhibits a larger peak-to-peak splitting between the anodic and cathodic waves, with a broad oxidation feature at 0.28 V and a reduction wave at -0.07 V versus $\text{Fc}^{+/0}$ (Figure S3). The different electrochemical behavior observed for **3** in the presence and absence of buffer is consistent with a process involving both proton and electron transfers.^{40,41}

Reactivity. Proton Transfer. The $\text{p}K_{\text{a}}$ of **3** was determined in CD₃CN by titration with bases of known $\text{p}K_{\text{a}}$ in CH₃CN (Scheme 1). A solution of pyridine in CD₃CN was titrated into a solution of **3** in CD₃CN, and the deprotonation reaction was monitored by ¹H NMR (Figure S8). An equilibrium mixture of **2** and **3** is rapidly established at 25 °C. As a result, only one set of ¹H NMR signals is observed for the Co complexes, which corresponds to the weighted average spectrum of **2** and **3**. Similarly, a rapid equilibrium is established between pyridine

Scheme 1. Titration of **3** with Pyridines (**B**) To Form **2** and Pyridinium Triflate (**BH**⁺)



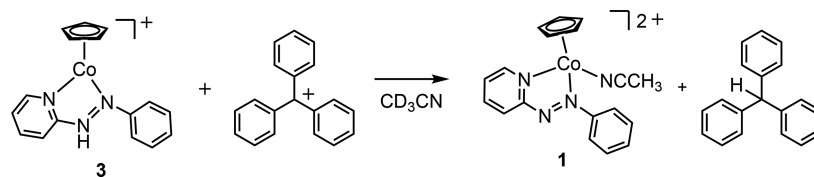
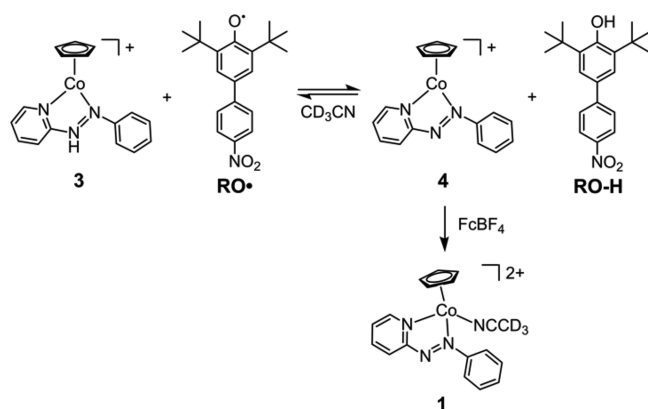
(**B**) and pyridinium (**BH**⁺), and a weighted average spectrum of this acid/base pair is observed. The concentrations of each species in solution were determined from the chemical shifts of the **2/3** and the **B/BH**⁺ signals, respectively. By this method, the equilibrium constant for this reaction is $K_{\text{eq}} = 64.3$. As the $\text{p}K_{\text{a}}$ of pyridine is 12.13 in acetonitrile,⁴² the $\text{p}K_{\text{a}}$ of **3** in acetonitrile is calculated to be 12.1 ± 0.1 . Analogous titrations of **3** with 2,6-lutidine ($\text{p}K_{\text{a}} = 14.13$ in acetonitrile⁴²) yield $\text{p}K_{\text{a}}(\mathbf{3}) = 12.3 \pm 0.2$ (Figure S9); titration of **2** with 4-methoxyanilinium tetrafluoroborate ($\text{p}K_{\text{a}} = 11.86$ in acetonitrile⁴²) yield $\text{p}K_{\text{a}}(\mathbf{3}) = 12.08 \pm 0.02$ (Figure S10). DFT calculations of the standard state free energy of proton transfer to 2,6-lutidine (see Computational Details) yield a comparable value, $\text{p}K_{\text{a, calc}}(\mathbf{3}) = 11$.

Hydride Transfer. The ability of **3** to function as a hydride donor was probed by examining the reaction of **3** with the triphenylcarbenium (trityl) cation (Scheme 2), which has a known hydricity of $\Delta G_{\text{H}^-} = 99$ kcal/mol in acetonitrile.^{19,43} Treatment of **3** with one equivalent of trityl tetrafluoroborate in CD₃CN leads to formation of **2** and triphenylmethane accompanied by some decomposition (Figure S11). Product formation was monitored by ¹H NMR, and the conversion of **3** with time is well described by a first order exponential decay (Figure S12). The half-life of this reaction is ca. 11 min at 25 °C, which corresponds to a rate constant of approximately $k_{\text{obs}} = 4.0 \text{ h}^{-1}$.

While hydride transfer from **3** to the trityl cation is too exergonic to experimentally measure the reaction free energy by ¹H NMR, an upper limit of $\Delta G_{\text{rxn}} = -3.7$ kcal/mol can be estimated based on the starting concentrations of **3** and the trityl cation, which gives that the hydricity of **3** is less than $\Delta G_{\text{H}^-} < 95$ kcal/mol. To gain a better estimate for the hydricity of **3**, the free energy of hydride transfer from **3** to the 1,3-dimethyl-1H-benzimidazolium cation (**BzIm**⁺) was calculated by DFT (see Computational Details). From the reported hydricity of 1,3-dimethyl-2H-benzimidazole (**BzImH**) in acetonitrile,⁴³ the calculated free energy for this reaction is 45.7 kcal/mol, leading to a calculated estimate for the hydricity of **3** of $\Delta G_{\text{H}^-}^{\text{(DFT)}} = 89$ kcal/mol. This value is comparable to that (88.7 kcal/mol) calculated from thermochemical cycles (see Discussion Section).

Hydrogen Atom Transfer. To assess the ability of **3** to function as a hydrogen atom donor, complex **3** was treated with one equivalent of the 2,6-di-*tert*-butyl-4-(4'-nitrophenyl)phenoxy radical (**RO**[•]). This reaction proceeds rapidly at room temperature. Analysis by ¹H NMR reveals the formation of the phenol **RO-H**, consistent with hydrogen atom transfer from **3** to the phenoxy radical (Scheme 3, Figures S13 and S14). According to Scheme 3, hydrogen atom transfer from **3** would form a monocationic Co(II) complex [CpCo(azpy)]⁺ **4**.³³ To provide evidence for the formation of this paramagnetic Co(II) species, the reaction mixture was treated with one equivalent of ferrocenium tetrafluoroborate (FcBF₄) as a chemical oxidant. Because the potential for the two-electron oxidation of **2** to **1** is -0.16 V versus $\text{Fc}^{+/0}$,³³ the ferrocenium cation should be sufficiently oxidizing to convert **4** into the diamagnetic Co(III) complex **1**. Analysis of the resulting mixture by ¹H NMR provides clear evidence for the quantitative formation of **1** (Figures S13 and S14), which indirectly supports the initial formation of **4** from the hydrogen atom transfer from **3** to the phenoxy radical. Because the phenol **RO-H** has an O–H homolytic bond dissociation free energy (BDFE) of $\Delta G_{\text{H}^\bullet} = 77.8$ kcal/mol in acetonitrile,⁴⁴ the

Scheme 2. Hydride Transfer from 3 to Trityl Tetrafluoroborate

Scheme 3. Hydrogen Atom Transfer from 3 to RO•, Followed by Oxidation of the Resulting Co^{II} species 4 with Ferrocenium Tetrafluoroborate To Form 1

results of this experiment suggest that the BDFE of the N–H bond of 3 is less than 78 kcal/mol.

The calculated reaction free energy for hydrogen atom transfer between 3 and RO• was found by DFT to be $\Delta G_{\text{rxn}} = -6.8$ kcal/mol (see [Computational Details](#)), which predicts that the homolytic N–H bond strength of 3 is $\Delta G_{\text{H}\cdot}^{\circ}(\text{DFT}) = 70.7$ kcal/mol. This value is comparable to that (67.7 kcal/mol) calculated from thermochemical cycles (see [Discussion Section](#))

DISCUSSION

Treatment of [CpCo(azpy)] 2 with strong acids such as *N,N*-dimethylformamidinium triflate readily yields [CpCo(azpyH)]⁺ 3. Characterization by low temperature ¹H NMR spectroscopy, solid state IR spectroscopy, and X-ray crystallography confirm that the added proton is localized on the azo nitrogen rather than the Co center.^{45,46} It is noteworthy that protonation exclusively occurs at the azo nitrogen of the azopyridine ligand given that protonation of the related [CpCo(dppe)] complex occurs at the metal center to form a Co(III)-H⁴⁵ and protonation of Cp*Rh(bipy) occurs at the Cp* ligand.^{47,48} Protonation at the azopyridine is attributed to the presence of a basic nitrogen on the ligand and a delocalized electronic structure of 2³³ where significant π -backbonding from the low valent cobalt center to the azopyridine ligand in 2 significantly decreases the basicity of the metal compared to other CpCoL₂ complexes bearing phosphine ligands.^{45,46,49} DFT calculations predict that protonation of the ligand is favored over protonation at the metal by 15 kcal/mol.

The protonated Co complex 3 exhibits a broad range of hydrogen transfer reactivity, acting as a proton donor, a hydride donor, and a hydrogen atom donor ([Figure 5](#)). Similar behavior has been demonstrated for a variety of transition metal hydrides⁵ as well as organic molecules,²⁶ but the electronic communication between the azopyridine ligand and

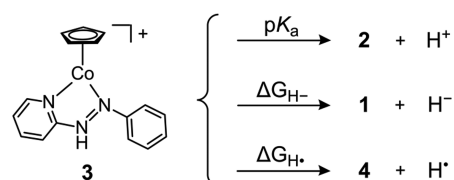


Figure 5. Reactivity of 3 as a proton, hydride, or hydrogen atom donor.

the Co center in this system has a significant influence on the thermodynamics of these hydrogen transfer reactions.

Complex 3 is a mildly strong acid, having $pK_a = 12.1$ in acetonitrile. The pK_a of 3 is significantly lower than that of acetic and benzoic acid (23.5 and 21.5, respectively), and is comparable to the acidities of monocationic N–H anilinium and pyridinium acids.⁵⁰ The relatively high acidity of 3 is attributed to the large stabilization of the conjugate base 2 from extensive delocalization across the metal and azopyridine ligand orbitals.³³ Complex 3 is more acidic than the Co(III)-hydride [CpCo(dppe)H]⁺ (dppe = 1,2-bis-(diphenylphosphino)ethane, $pK_a(\text{CH}_3\text{CN}) = 18.4$).⁴⁶ As a comparison, the pK_a values of [CpM(CO)₃H] (M = Cr, Mo, and W) are between 13.3 and 16.1, and the pK_a of [(C₆H₆)Ru(bipy)H]⁺ is 23 in acetonitrile.⁵¹

The pK_a of 3 can be used in combination with its electrochemical properties to calculate the thermodynamics of heterolytic and homolytic cleavage of the N–H bond. The heterolytic bond dissociation energy, or hydricity $\Delta G_{\text{H}^-}^{\circ}$, of an X–H bond can be estimated from the acidity (pK_a) and two-electron oxidation potential (E°) of the conjugate base in acetonitrile.^{43,52} For complex 3, hydricity is given by [eq 1](#).

$$\begin{aligned} \Delta G_{\text{H}^-}^{\circ}(\text{kcal/mol}) \\ = 1.364 pK_a(3) + 46.12 E^{\circ}(2/1) + 79.6 \end{aligned} \quad (1)$$

From the pK_a of the N–H bond and the two-electron oxidation potential of 2, [eq 1](#), the hydricity of 3 is estimated to be $\Delta G_{\text{H}^-}^{\circ} = 88.7$ kcal/mol in acetonitrile, which is in good agreement with the DFT-calculated value ($\Delta G_{\text{H}^-}^{\circ}(\text{DFT}) = 89$ kcal/mol). Hydride transfer from 3 will be thermodynamically favorable when the hydride donating ability of 3 is greater than that of the substrate. Because there are few substrates with weaker hydride donating abilities than 3, this complex is considered a poor thermodynamic hydride donor. Indeed, the hydride donating ability of 3 is lower than all known values for transition metal hydrides in acetonitrile.⁴ The hydricity of 3 is similar to that of various substituted NADH analogues and triarylmethanes.⁵³ Hydride transfer from 3 to the trityl cation is successful because the hydride donating ability of triphenylmethane is even worse than that of 3 ($\Delta G_{\text{H}^-} = 99$ kcal/mol versus 89 kcal/mol in acetonitrile, respectively). While this reaction has a large driving force of 10 kcal/mol, this hydride transfer took 2 h to reach completion, demonstrating that 3 is a

poor hydride donor from both a kinetic and thermodynamic standpoint.

The homolytic bond dissociation free energy (BDFE or $\Delta G^\circ_{\text{H}\cdot}$) of an X–H bond can be calculated from the acidity ($\text{p}K_{\text{a}}$) and the one-electron oxidation potential (E°) of the conjugate base in acetonitrile (eq 2).^{2,54} For complex **3**, the BDFE is given by eq 2.

$$\Delta G^\circ_{\text{H}\cdot}(\text{kcal/mol}) = 1.364 \text{p}K_{\text{a}}(\mathbf{3}) + 23.06 E^\circ(\mathbf{2}/\mathbf{4}) + 54.9 \quad (2)$$

Applying eq 2 with the $\text{p}K_{\text{a}}$ of **3** and the oxidation potential of **2** in acetonitrile yields an estimated BDFE of the N–H bond of 67.7 kcal/mol, which is in close agreement with the DFT-calculated value ($\text{BDFE}_{\text{calc}} = 70.7 \text{ kcal/mol}$). We note that because **2** exhibits a reversible two-electron oxidation to **1**, the one-electron oxidation potential of **2** to **4** in eq 2 is taken to be equivalent to the potential of this two-electron process, which does introduce some error to this estimated BDFE value.

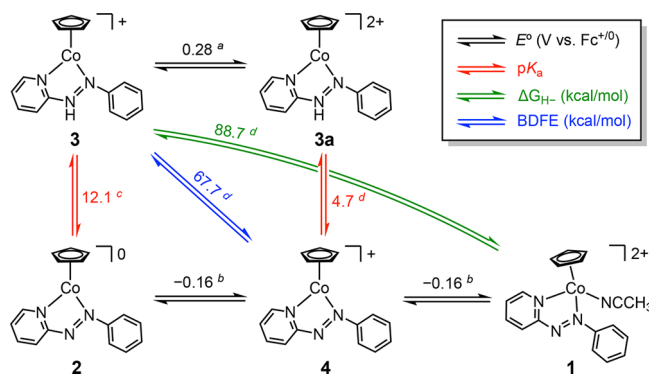
The reaction of **3** with the phenoxyl radical $\text{RO}\cdot$ to yield the corresponding phenol RO-H ($\text{BDFE}(\text{CH}_3\text{CN}) = 77.8 \text{ kcal/mol}$)⁴⁴ is consistent with the lower estimated BDFE for **3** relative to that of RO-H . As the protonated phenoxyl radical $\text{RO-H}^{+\cdot}$ is likely very acidic ($\text{p}K_{\text{a}} \approx 0.14$ in acetonitrile),⁴⁴ initial proton transfer from **3** ($\text{p}K_{\text{a}} = 12.1$) is not likely. Initial electron transfer from **1** ($E_{\text{ox}} = 0.28 \text{ V}$) to $\text{RO}\cdot$ ($E_{\text{red}} = -0.436 \text{ V}$) is also not thermodynamically favorable; therefore, the reaction of **3** with $\text{RO}\cdot$ is most consistent with hydrogen atom transfer. The large negative free energy for this reaction precluded an experimental measure for the BDFE of **3**. Attempts to observe hydrogen atom transfer from **3** to nitroxyl radicals having lower BDFEs (e.g., TEMPO radical) were complicated by coordination of the radicals and hydroxylamines to **1** and additional proton transfers following hydrogen atom transfer.

The BDFE of **3** is slightly higher than that of other cyclopentadienyl metal hydride complexes $[\text{CpM}(\text{CO})_3\text{H}]$ ($\text{M} = \text{Cr, Mo, or W}$), $[\text{CpM}(\text{CO})_2\text{H}]$ ($\text{M} = \text{Fe or Ru}$), and $[\text{M}(\text{CO})_5\text{H}]$ complexes ($\text{M} = \text{Mn, Re}$), which have BDFE values between 51 and 65 kcal/mol.² Mayer^{15,16,18} and others²⁶ have studied a variety of metal complexes in which a net hydrogen atom transfer occurs through coupled electron transfer from a redox-active metal and proton transfer from a proton-active ligand. We posit that hydrogen atom transfer from **3** proceeds analogously: proton transfer from the N–H bond is coupled with electron transfer from the low valent Co(I) center to achieve net hydrogen atom transfer with concomitant formation of the Co(II) complex **4**. The estimated BDFE of **3** falls in the same range as the Fe^{II} and Co^{II} biimidazoline complexes (ca. 65–70 kcal/mol in acetonitrile) that exhibit this reactivity.^{15,18} Notably, the octahedral cobalt biimidazoline system described by Mayer¹⁸ is a kinetically poor hydrogen atom donor due to the spin-forbidden conversion from the reactants (high-spin quartet $\text{Co(II)} + \text{doublet TEMPO radical}$) to products (low-spin singlet $\text{Co(III)} + \text{singlet TEMPO-H}$) upon hydrogen atom transfer. The conversion of high-spin Co(II) to low-spin Co(III) is associated with a large inner-sphere reorganization energy, leading to a kinetic barrier to hydrogen atom transfer. In contrast, hydrogen atom transfer from low-spin **3** generates **4**, which is predicted by DFT to be low-spin Co(II) due to the strong ligand field of the azopyridine ligand.³³ Therefore, no

initial spin conversion is required for hydrogen atom transfer from **3**.

The relationships between the redox potentials and the homolytic and heterolytic bond dissociation free energies for **3** can be displayed in a thermochemical square scheme as shown in Scheme 4. Here, oxidation potentials (in V versus $\text{Fc}^{+/0}$) are

Scheme 4. Thermochemical Square Scheme for **3 in Acetonitrile**



^aIrreversible two-electron-one-proton oxidation potential. ^bTwo-electron redox potential. ^cExperimentally determined via titration experiments. ^dDetermined via thermochemical square-scheme analysis.

given by the black horizontal arrows, $\text{p}K_{\text{a}}$ values are given by the red vertical arrows, BDFE (in kcal/mol) is given by the blue diagonal arrow, and hydricity (in kcal/mol) is given by the curved green arrow. Because these parameters are all state functions, the sum of any combination of reactions may be used to describe a particular bond cleavage reaction. Therefore, it follows that the acidity of **3** plus the one-electron oxidation potential of **2** must equal the sum of the acidity of **3a** plus the one-electron oxidation potential of **3**, as shown in eq 3.

$$1.364 \text{p}K_{\text{a}}(\mathbf{3}) + 23.06 E^\circ(\mathbf{2}/\mathbf{4}) = 1.364 \text{p}K_{\text{a}}(\mathbf{3a}) + 23.06 E^\circ(\mathbf{3}/\mathbf{3a}) \quad (3)$$

Though not determined experimentally, the acidity of the protonated dicationic complex **3a** can be estimated using eq 3. Using the measured values for the relevant $\text{p}K_{\text{a}}$ and electrochemical data, the $\text{p}K_{\text{a}}$ of **3a** is calculated to be approximately 4.7 in acetonitrile. We note that this value is a very crude approximation for the $\text{p}K_{\text{a}}$ of **3a** because the experimental values used for $E^\circ(\mathbf{3}/\mathbf{3a})$ and $E^\circ(\mathbf{2}/\mathbf{4})$ represent two-electron-one-proton and two-electron oxidation processes, respectively, rather than reversible one-electron redox couples. Based on this scheme and eq 1, it is clear that the poor hydride donating ability of **3** is a direct result of the unusually high stability of the neutral complex **2**, which stems from the optimal energy matching of the cobalt metal and azopyridine ligand orbitals.³³ The stability of **2** gives rise to the relatively high acidity of the N–H bond in **3** and the mild oxidation potential required for the two-electron oxidation of **2** and **1**. Moreover, by Scheme 4 and eq 2, the relatively weak BDFE of **3** is similarly explained by the acidity of **3** and the mild oxidation potential of **2**, further highlighting the unique role of the extensive cobalt-azopyridine orbital overlap in **2**³³ for governing the reactivity of this N–H bond.

CONCLUSION

Treatment of the neutral azopyridine complex [CpCo(azpy)] **2** with strong acid results in protonation at the azo ligand rather than the cobalt center to generate **3**, which has been isolated and characterized by spectroscopic and electrochemical methods. The thermodynamics of proton, hydrogen atom, and hydride donation from **3** have been explored. The N–H bond is reasonably acidic having $pK_a = 12.1$ in acetonitrile. Though **3** is a poor hydride donor, the large ΔG_{H-} (88.8 kcal/mol) suggests that **1** may function as a strong hydride acceptor with many substrates. The homolytic bond strength of the N–H is relatively weak (BDFE = 67.8 kcal/mol) and **3** readily reacts with a phenoxy radical (BDFE = 77.8 kcal/mol) via hydrogen atom transfer. Notably, the mild conditions at which the different protonation and redox states of this system can be interconverted are attractive for hydrogen transfer reactions, especially in the context of electrochemical hydrogen atom transfer. Studies exploring this reactivity are currently underway.

EXPERIMENTAL SECTION

Materials. All experiments were carried out under a nitrogen or argon atmosphere using standard vacuum line, Schlenk, and glovebox techniques. Solvents were dried following standard methods and degassed via three freeze–pump–thaw cycles. Deuterated solvents for NMR were purchased from Cambridge Isotope Laboratories. All reagents were used as received unless otherwise described. Tetrabutylammonium perchlorate (Sigma-Aldrich) was recrystallized from ethanol, dried under reduced pressure, and stored in an inert atmosphere glovebox. Ferrocene (Sigma-Aldrich) was sublimed under vacuum and stored in an inert atmosphere glovebox. Acetylferrocene (Sigma-Aldrich) was recrystallized from hexanes, dried under reduced pressure, and stored in an inert atmosphere glovebox. The synthesis of the [CpCo(azpy)(CH₃CN)] [ClO₄]₂ **1**,³³ CpCo(azpy) **2**,³³ ^tBu₂NPArO,⁴⁴ and [DMFH][CF₃SO₃]⁵⁵ have been described previously. **CAUTION:** While we experienced no difficulties with the use of perchlorate salts, they should be regarded as potentially explosive and handled with care.

Instrumentation. ¹H and ¹³C NMR spectra were recorded on Varian 300, 400, or 500 MHz spectrometers. All NMR spectra were taken at room temperature unless stated otherwise. Residual solvent proton and carbon peaks were used as reference. Chemical shifts are reported in parts per million (δ). IR spectra were recorded as solids using an attenuated total reflectance FT-IR spectrophotometer.

Electrochemical experiments were performed using a WaveNow USB Potentiostat (Pine Research Instrumentation) at ambient temperature in an inert atmosphere glovebox. For cyclic voltammetry, the electrochemical cell consisted of a three-electrode setup using a glassy carbon working electrode (3 mm diameter, Bioanalytical Systems, Inc.), platinum auxiliary electrode, and Ag/AgNO₃ non-aqueous reference electrode (Bioanalytical Systems, Inc.). The glassy carbon electrode was polished between each scan. All potentials are referenced to the Fc^{+/0} couple (0.0 V) using acetylferrocene (0.25 V versus Fc^{+/0}) as an internal reference. All electrochemical experiments were performed with 0.1 M tetrabutylammonium perchlorate supporting electrolyte in acetonitrile.

X-ray Crystallography. Single crystals for X-ray analysis were mounted on a Kapton loop using Paratone N hydrocarbon oil or perfluorinated ether oil. All measurements were made on a Bruker APEX II CCD detector X-ray diffractometer with graphite monochromated Mo K α radiation ($\lambda = 0.71073$ Å). Frames corresponding to an arbitrary sphere of data were collected using ω -scans of 0.3° counted for a total of 10 s per frame. Data were integrated using the Bruker SAINT software program⁵⁶ to a maximum θ -value of 28.26°, analyzed for agreement and possible absorption using XPR,⁵⁷ and corrected for Lorentz and polarization effects. Absorption corrections were applied using the SADABS program.⁵⁶

No decay correction was applied. Structures were solved by direct methods,⁵⁶ expanded using Fourier techniques, and refined by full-matrix least-squares procedures based on F².⁵⁸ Hydrogen atoms were included in ideal positions and refined isotropically in riding model with Uiso = 1.5Ueq(X) for methyl groups and Uiso = 1.2Ueq(X) for other atoms, where Ueq(X) are thermal parameters of parent atoms. Non-hydrogen atoms were refined anisotropically. Crystals of **3** suitable for X-ray diffraction were obtained from vapor diffusion of diethyl ether into an acetonitrile solution. Crystallographic data is presented in the [Supporting Information](#).

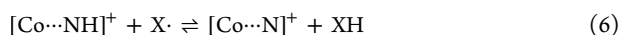
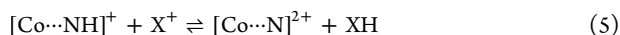
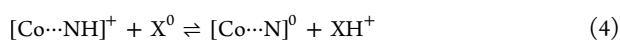
Synthesis. [CpCo(azpyH)][CF₃SO₃] **3**. A solution of [DMFH][CF₃SO₃] (22 mg, 0.099 mmol) in benzene (5 mL) was added dropwise to a solution of CpCo(azpy) **2** (30 mg, 0.098 mmol) in benzene (5 mL) while stirring under N₂. The solution was stirred under N₂ at room temperature for 30 min. The dark red solid that precipitated from solution was collected via filtration and washed thoroughly with benzene. ¹H NMR (500 MHz, CD₃CN): δ 12.10 (s, 1H), 10.22 (d, $J = 6.4$ Hz, 1H), 8.13 (d, $J = 7.4$ Hz, 2H), 7.61 (d, $J = 8.6$ Hz, 1H), 7.48–7.42 (m, 3H), 7.36 (ddd, $J = 8.5, 6.9, 1.5$ Hz, 1H), 6.98 (td, $J = 6.5, 1.3$ Hz, 1H), 4.84 (s, 5H).

Reactivity Studies. Representative Procedure for pK_a Titrations with **3.** A stock solution of pyridine (5 μ L in 0.5 mL CD₃CN, 0.123 M) and a stock solution of hexamethylbenzene (HMB) (3.1 mg in 0.6 mL CD₃CN, 0.032 M) were prepared in an inert atmosphere glovebox. In a sealable NMR tube, 40 μ L of the HMB stock solution was added to a solution of **3** (1.9 mg in 0.5 mL CD₃CN, 0.0083 M). Upon recording a ¹H NMR spectrum of this solution, 10 μ L of the pyridine stock solution was added and another ¹H NMR spectrum was recorded. This procedure was repeated for an additional three 10 μ L aliquots, three 20 μ L aliquots, and a 50 μ L aliquot.

Hydride Transfer from **3 to Trityl Cation.** A solution of [CpCo(azpy)] **2** in CD₃CN was prepared in an inert atmosphere glovebox (1.0 mg in 0.5 mL, 0.0054 M). Outside the box, 0.015 mL of trifluoromethanesulfonic acid (TfOH) solution (0.224 M in CD₃CN) was added and a ¹H NMR spectrum was acquired. Upon confirming the formation of **3**, 0.105 mL of trityl tetrafluoroborate solution (5.0 mg in 0.5 mL CD₃CN, 0.0303 M) was added. Conversion of **3** and formation of triphenylmethane was monitored by ¹H NMR.

Hydrogen Atom Transfer from **3 to ^tBu₂NPArO.** A solution of [CpCo(azpy)] **2** in C₆D₆ (1.9 mg in 0.4 mL, 0.016 M) was added to a solution of [DMFH][CF₃SO₃] in C₆D₆ (1.4 mg in 0.4 mL, 0.016 M). The solution was stirred at room temperature under N₂ for 10 min, after which time the solution was decanted via syringe. The remaining precipitate was dissolved in 0.4 mL CD₃CN and treated with ^tBu₂NPArO in 0.4 mL CD₃CN (2.0 mg, 0.0062 mmol). The solution was sonicated for 15 min and the ¹H NMR spectrum was recorded. Upon disappearance of **3** and appearance of ^tBu₂NPArOH, ferrocenium tetrafluoroborate (1.7 mg, 0.0062 mmol) was added. The solution was sonicated for 15 min and the ¹H NMR was recorded.

Computational Details. All Kohn–Sham density functional theory-based calculations^{59–61} were done using the Gaussian 09 (G09), revision D.01,⁶² software package, using the BP86 functional^{63,64} in combination with the TZVP⁶⁵ basis set on all atoms. The structures were optimized in the gas phase on an ultrafine grid using the “tight” convergence criterion as implemented in G09. This was followed by a harmonic analysis of the stationary point to yield force constants, which were then used to estimate standard state free energies (1 atm, 298 K). Solvation free energies were determined using the polarizable continuum “SMD” model⁶⁶ for acetonitrile. The reaction free energies for the three N–H cleavage modes of **3** were computed as shown in eqs 4–6. Standard state corrections were made to the free energies in order to account for the change in going from 1 mol per 24.46 L (gas phase) to 1 M (solution phase). For the stoichiometric gain of an acetonitrile ligand (during hydride transfer), a correction of $-RT\ln(19.15) = 1.75$ kcal/mol was applied to the free energy. Cartesian coordinates for **1**, **2**, and **4** have been previously reported.³³ Cartesian coordinates for all other reactants and products are given in the [Supporting Information](#).



■ ASSOCIATED CONTENT

Supporting Information

The Supporting Information is available free of charge on the ACS Publications website at DOI: [10.1021/jacs.8b06156](https://doi.org/10.1021/jacs.8b06156).

Tabulated X-ray data, and molecular structure obtained from single crystal X-ray diffraction; additional cyclic voltammograms, ^1H NMR titration experiments, hydride transfer studies, hydrogen atom transfer studies, and Cartesian coordinates of DFT-optimized reactants and products (PDF)

Crystallographic data file (CIF)

■ AUTHOR INFORMATION

Corresponding Author

*waymouth@stanford.edu

ORCID

Elizabeth A. McLoughlin: 0000-0003-1481-266X

Kate M. Waldie: 0000-0001-6444-6122

Srinivasan Ramakrishnan: 0000-0003-3204-8095

Robert M. Waymouth: 0000-0001-9862-9509

Author Contributions

[†]These authors contributed equally.

Notes

The authors declare no competing financial interest.

■ ACKNOWLEDGMENTS

This material is based on work supported by the Global Climate and Energy Program at Stanford and the National Science Foundation (CHE-1565947). E.A.M. and K.M.W. are grateful for Center for Molecular Analysis and Design (CMAD) Fellowships. K.M.W. is grateful for a Gabilan Stanford Graduate Fellowship and National Science and Engineering Research Council of Canada (NSERC) Post-graduate Scholarship.

■ REFERENCES

- Zhu, X. Q.; Zhang, M. T.; Yu, A.; Wang, C. H.; Cheng, J. P. Hydride, hydrogen atom, proton, and electron transfer driving forces of various five-membered heterocyclic organic hydrides and their reaction intermediates in acetonitrile. *J. Am. Chem. Soc.* **2008**, *130*, 2501–2516.
- Warren, J. J.; Tronic, T. A.; Mayer, J. M. Thermochemistry of Proton-Coupled Electron Transfer Reagents and its Implications. *Chem. Rev.* **2010**, *110*, 6961–7001.
- Weinberg, D. R.; Gagliardi, C. J.; Hull, J. F.; Murphy, C. F.; Kent, C. A.; Westlake, B. C.; Paul, A.; Ess, D. H.; McCafferty, D. G.; Meyer, T. J. Proton-coupled electron transfer. *Chem. Rev.* **2012**, *112*, 4016–4093.
- Wiedner, E. S.; Chambers, M. B.; Pitman, C. L.; Bullock, R. M.; Miller, A. J.; Appel, A. M. Thermodynamic Hydricity of Transition Metal Hydrides. *Chem. Rev.* **2016**, *116*, 8655–8692.
- Hu, Y.; Norton, J. R. Kinetics and Thermodynamics of H-/H center dot/H+ Transfer from a Rhodium(III) Hydride. *J. Am. Chem. Soc.* **2014**, *136*, 5938–5948.
- Hartung, J.; Norton, J. R. In *Catalysis without Precious Metals*; Bullock, R. M., Ed.; Wiley-VCH: Weinheim, 2010; pp 1–24.
- Eisenberg, D. C.; Norton, J. R. Hydrogen-Atom Transfer Reactions of Transition-Metal Hydrides. *Isr. J. Chem.* **1991**, *31*, 55–66.
- Baldwin, M. J.; Pecoraro, V. L. Energetics of Proton-Coupled Electron Transfer in High-Valent $\text{Mn}_2(\mu\text{-O})_2$ Systems: Models for Water Oxidation by the Oxygen-Evolving Complex of Photosystem II. *J. Am. Chem. Soc.* **1996**, *118*, 11325–11326.
- Caudle, M. T.; Pecoraro, V. L. Thermodynamic Viability of Hydrogen Atom Transfer from Water Coordinated to the Oxygen-Evolving Complex of Photosystem II. *J. Am. Chem. Soc.* **1997**, *119*, 3415–3416.
- Gupta, R.; MacBeth, C. E.; Young, V. G.; Borovik, A. S. Isolation of monomeric Mn(III/II)-OH and Mn(III)-O complexes from water: evaluation of O-H bond dissociation energies. *J. Am. Chem. Soc.* **2002**, *124*, 1136–1137.
- Waidmann, C. R.; Zhou, X.; Tsai, E. A.; Kaminsky, W.; Hrovat, D. A.; Borden, W. T.; Mayer, J. M. Slow hydrogen atom transfer reactions of oxo- and hydroxo-vanadium compounds: The importance of intrinsic barriers. *J. Am. Chem. Soc.* **2009**, *131*, 4729–4743.
- Soper, J. D.; Mayer, J. M. Slow Hydrogen Atom Self-Exchange between Os(IV) Anilide and Os(III) Aniline Complexes: Relationships with Electron and Proton Transfer Self-Exchange. *J. Am. Chem. Soc.* **2003**, *125*, 12217–12229.
- Leung, S. K.-Y.; Tsui, W.-M.; Huang, J.-S.; Che, C.-M.; Liang, J.-L.; Zhu, N. Imido transfer from bis(imido)ruthenium(VI) porphyrins to hydrocarbons: Effect of imido substituents, C-H bond dissociation energies, and Ru VI/V reduction potentials. *J. Am. Chem. Soc.* **2005**, *127*, 16629–16640.
- Eckert, N. A.; Vaddadi, S.; Stoian, S.; Lachicotte, R. J.; Cundari, T. R.; Holland, P. L. Coordination-number dependence of reactivity in an imidoiron(III) complex. *Angew. Chem., Int. Ed.* **2006**, *45*, 6868–6871.
- Roth, J. P.; Lovell, S.; Mayer, J. M. Intrinsic Barriers for Electron and Hydrogen Atom Transfer Reactions of Biomimetic Iron Complexes. *J. Am. Chem. Soc.* **2000**, *122*, 5486–5498.
- Roth, J. P.; Yoder, J. C.; Won, T.-J.; Mayer, J. M. Application of the Marcus Cross Relation to Hydrogen Atom Transfer Reactions. *Science* **2001**, *294*, 2524–2526.
- Wu, A.; Masland, J.; Swartz, R. D.; Kaminsky, W.; Mayer, J. M. Synthesis and Characterization of Ruthenium Bis(B-diketonato) Pyridine-Imidazole Complexes for Hydrogen Atom Transfer. *Inorg. Chem.* **2007**, *46*, 11190–11201.
- Manner, V. W.; Lindsay, A. D.; Mader, E. A.; Harvey, J. N.; Mayer, J. M. Spin-forbidden hydrogen atom transfer reactions in a cobalt biimidazole system. *Chem. Sci.* **2012**, *3*, 230–243.
- Eisenberg, D. C.; Lawrie, C. J. C.; Moody, A. E.; Norton, J. R. Relative Rates of H. Transfer from Transition-Metal Hydrides to Trityl Radicals. *J. Am. Chem. Soc.* **1991**, *113*, 4888–4895.
- Nibbering, E. T. J.; Pines, E. In *Hydrogen-Transfer Reactions*; Wiley-VCH: Weinheim, 2007; pp 443–458.
- Kubas, G. J. In *Hydrogen-Transfer Reactions*; Wiley-VCH: Weinheim, 2007; pp 603–637.
- Schöneich, C. In *Hydrogen-Transfer Reactions*; Wiley-VCH: Weinheim, 2007; pp 1013–1035.
- Schowen, R. L. In *Hydrogen-Transfer Reactions*; Wiley-VCH: Weinheim, 2007; pp 1037–1077.
- Hodgkiss, J. M.; Rosenthal, J.; Nocera, D. G. In *Hydrogen-Transfer Reactions*; Wiley-VCH: Weinheim, 2007; pp 503–562.
- Elgrishi, N.; McCarthy, B. D.; Rountree, E. S.; Dempsey, J. L. Reaction pathways of hydrogen-evolving electrocatalysts: electrochemical and spectroscopic studies of proton-coupled electron transfer processes. *ACS Catal.* **2016**, *6*, 3644–3659.
- McSkimming, A.; Colbran, S. B. The coordination chemistry of organo-hydride donors: new prospects for efficient multi-electron reduction. *Chem. Soc. Rev.* **2013**, *42*, 5439–5488.
- Ghosh, D.; Kobayashi, K.; Kajiwara, T.; Kitagawa, S.; Tanaka, K. Catalytic Hydride Transfer to CO_2 Using Ru-NAD-Type Complexes under Electrochemical Conditions. *Inorg. Chem.* **2017**, *56*, 11066–11073.

- (28) Koizumi, T.; Tanaka, K. Reversible hydride generation and release from the ligand of Ru(pbn)(bpy)(2) (PF6)(2) driven by a pbn-localized redox reaction. *Angew. Chem., Int. Ed.* **2005**, *44*, 5891–5894.
- (29) Ohtsu, H.; Tanaka, K. An Organic Hydride Transfer Reaction of a Ruthenium NAD Model Complex Leading to Carbon Dioxide Reduction. *Angew. Chem., Int. Ed.* **2012**, *51*, 9792–9795.
- (30) Padhi, S. K.; Fukuda, R.; Ehara, M.; Tanaka, K. Comparative Study of (CN)-N-boolean AND and (NC)-C-boolean AND Type Cyclometalated Ruthenium Complexes with a NAD(+)/NADH Function. *Inorg. Chem.* **2012**, *51*, 8091–8102.
- (31) Wilting, A.; Kugler, M.; Siewert, I. Copper Complexes with NH-Imidazolyl and NH-Pyrazolyl Units and Determination of Their Bond Dissociation Gibbs Energies. *Inorg. Chem.* **2016**, *55*, 1061–1068.
- (32) Chirik, P. J.; Wieghardt, K. Radical ligands confer nobility on base-metal catalysts. *Science* **2010**, *327*, 794–795.
- (33) Waldie, K. M.; Ramakrishnan, S.; Kim, S.-K.; Maclaren, J. K.; Chidsey, C. E. D.; Waymouth, R. M. Multielectron Transfer at Cobalt: Influence of the Phenylazopyridine Ligand. *J. Am. Chem. Soc.* **2017**, *139*, 4540–4550.
- (34) Sanyal, A.; Banerjee, P.; Lee, G.-H.; Peng, S.-M.; Hung, C.-H.; Goswami, S. Unusual reduction of ammonium heptamolybdate to novel molybdenum (IV)-stabilized azo anion radical complexes. *Inorg. Chem.* **2004**, *43*, 7456–7462.
- (35) Sanyal, A.; Chatterjee, S.; Castineiras, A.; Sarkar, B.; Singh, P.; Fiedler, J.; Zális, S.; Kaim, W.; Goswami, S. Singlet diradical complexes of chromium, molybdenum, and tungsten with azo anion radical ligands from M (CO) 6 precursors. *Inorg. Chem.* **2007**, *46*, 8584–8593.
- (36) Joy, S.; Krämer, T.; Paul, N. D.; Banerjee, P.; McGrady, J. E.; Goswami, S. Isolation and Assessment of the Molecular and Electronic Structures of Azo-Anion-Radical Complexes of Chromium and Molybdenum. Experimental and Theoretical Characterization of Complete Electron-Transfer Series. *Inorg. Chem.* **2011**, *50*, 9993–10004.
- (37) Paul, N. D.; Rana, U.; Goswami, S.; Mondal, T. K.; Goswami, S. Azo Anion Radical Complex of Rhodium as a Molecular Memory Switching Device: Isolation, Characterization, and Evaluation of Current–Voltage Characteristics. *J. Am. Chem. Soc.* **2012**, *134*, 6520–6523.
- (38) Ghosh, P.; Samanta, S.; Roy, S. K.; Joy, S.; Krämer, T.; McGrady, J. E.; Goswami, S. Redox Noninnocence in Coordinated 2-(Arylazo) pyridines: Steric Control of Ligand-Based Redox Processes in Cobalt Complexes. *Inorg. Chem.* **2013**, *52*, 14040–14049.
- (39) Waldie, K. M.; Kim, S.-K.; Ingram, A. J.; Waymouth, R. M. Cyclopentadienyl Cobalt Complexes as Precatalysts for Electrocatalytic Hydrogen Evolution. *Eur. J. Inorg. Chem.* **2017**, *2017*, 2755–2761.
- (40) Takeuchi, K. J.; Thompson, M. S.; Pipes, D. W.; Meyer, T. J. Redox and Spectral Properties of Monooxo Polypyridyl Complexes of Ruthenium and Osmium in Aqueous-Media. *Inorg. Chem.* **1984**, *23*, 1845–1851.
- (41) Gerli, A.; Reedijk, J.; Lakin, M. T.; Spek, A. L. Redox Properties and Electrocatalytic Activity of the Oxo/Aqua System [Ru (terpy)-(bpz)(O)] 2+/[Ru (terpy)(bpz)(H2O)] 2+. X-ray Crystal Structure of [Ru (terpy)(bpz) Cl] PF6. cntdot. MeCN (terpy= 2, 2', 2''-Terpyridine; bpz= 2, 2'-Bipyrazine). *Inorg. Chem.* **1995**, *34*, 1836–1843.
- (42) Kaljurand, I.; Kütt, A.; Sooväli, L.; Rodima, T.; Mäemets, V.; Leito, I.; Koppel, I. A. Extension of the self-consistent spectrophotometric basicity scale in acetonitrile to a full span of 28 p K a units: unification of different basicity scales. *J. Org. Chem.* **2005**, *70*, 1019–1028.
- (43) Matsubara, Y.; Fujita, E.; Doherty, M. D.; Muckerman, J. T.; Creutz, C. Thermodynamic and kinetic hydricity of ruthenium(II) hydride complexes. *J. Am. Chem. Soc.* **2012**, *134*, 15743–15757.
- (44) Porter, T. R.; Kaminsky, W.; Mayer, J. M. Preparation, Structural Characterization, and Thermochemistry of an Isolable 4-Arylphenoxy Radical. *J. Org. Chem.* **2014**, *79*, 9451–9454.
- (45) Koelle, U.; Paul, S. Electrochemical reduction of protonated cyclopentadienylcobalt phosphine complexes. *Inorg. Chem.* **1986**, *25*, 2689–2694.
- (46) Elgrishi, N.; Kurtz, D. A.; Dempsey, J. L. Reaction Parameters Influencing Cobalt Hydride Formation Kinetics: Implications for Benchmarking H2-Evolution Catalysts. *J. Am. Chem. Soc.* **2017**, *139*, 239–244.
- (47) Quintana, L. M. A.; Johnson, S. I.; Corona, S. L.; Villatoro, W.; Goddard, W. A.; Takase, M. K.; VanderVelde, D. G.; Winkler, J. R.; Gray, H. B.; Blakemore, J. D. Proton–hydride tautomerism in hydrogen evolution catalysis. *Proc. Natl. Acad. Sci. U. S. A.* **2016**, *113*, 6409–6414.
- (48) Pitman, C. L.; Finster, O. N. L.; Miller, A. J. M. Cyclopentadiene-mediated hydride transfer from rhodium complexes. *Chem. Commun.* **2016**, *52*, 9105–9108.
- (49) Nagasawa, T.; Nagata, T. Synthesis and electrochemistry of Co(III) and Co(I) complexes having C5Me5 auxiliary. *Biochim. Biophys. Acta, Bioenerg.* **2007**, *1767*, 666–670.
- (50) McCarthy, B. D.; Martin, D. J.; Rountree, E. S.; Ullman, A. C.; Dempsey, J. L. Electrochemical Reduction of Brønsted Acids by Glassy Carbon in Acetonitrile-Implications for Electrocatalytic Hydrogen Evolution. *Inorg. Chem.* **2014**, *53*, 8350–8361.
- (51) Morris, R. H. Brønsted–Lowry acid strength of metal hydride and dihydrogen complexes. *Chem. Rev.* **2016**, *116*, 8588–8654.
- (52) Curtis, C. J.; Miedaner, A.; Ellis, W. W.; DuBois, D. L. Measurement of the hydride donor abilities of [HM(diphosphine)2]+ complexes (M = Ni, Pt) by heterolytic activation of hydrogen. *J. Am. Chem. Soc.* **2002**, *124*, 1918–1925.
- (53) Waldie, K. M.; Ostericher, A. L.; Reineke, M. H.; Sasayama, A. F.; Kubiak, C. P. Hydricity of Transition-Metal Hydrides: Thermodynamic Considerations for CO2 Reduction. *ACS Catal.* **2018**, *8*, 1313–1324.
- (54) Parker, V. D.; Handoo, K. L.; Roness, F.; Tilset, M. Electrode potentials and the thermodynamics ofisodesmic reactions. *J. Am. Chem. Soc.* **1991**, *113*, 7493–7498.
- (55) Favier, I.; Duñach, E. New protic salts of aprotic polar solvents. *Tetrahedron Lett.* **2004**, *45*, 3393–3395.
- (56) Sheldrick, G. M. A short history of SHELX. *Acta Crystallogr., Sect. A: Found. Crystallogr.* **2008**, *64*, 112–122.
- (57) XPREP: Part of the SHELXTL Crystal Structure Determination Package, v 6.14; Siemens Industrial Automation, Inc.: Madison, WI, 1995.
- (58) XL: Program for the Refinement of X-ray Crystal Structure, Part of the SHELXTL Crystal Structure Determination Package; Bruker Analytical X-ray Systems Inc.: Madison, WI, 1995–99.
- (59) Hohenberg, P.; Kohn, W. Inhomogeneous electron gas. *Phys. Rev.* **1964**, *136*, B864.
- (60) Kohn, W.; Sham, L. J. Self-consistent equations including exchange and correlation effects. *Phys. Rev.* **1965**, *140*, A1133.
- (61) Parr, R. G.; Weitao, Y. *Density-Functional Theory of Atoms and Molecules*; Oxford University Press: New York, 1994.
- (62) Frisch, M. J.; Trucks, G. W.; Schlegel, H. B.; Scuseria, G. E.; Robb, M. A.; Cheeseman, J. R.; Scalmani, G.; Barone, V.; Petersson, G. A.; Nakatsuji, H.; Li, X.; Caricato, M.; Marenich, A. V.; Bloino, J.; Janesko, B. G.; Gomperts, R.; Mennucci, B.; Hratchian, H. P.; Ortiz, J. V.; Izmaylov, A. F.; Sonnenberg, J. L.; Williams, Ding, F.; Lipparini, F.; Egidi, F.; Goings, J.; Peng, B.; Petrone, A.; Henderson, T.; Ranasinghe, D.; Zakrzewski, V. G.; Gao, J.; Rega, N.; Zheng, G.; Liang, W.; Hada, M.; Ehara, M.; Toyota, K.; Fukuda, R.; Hasegawa, J.; Ishida, M.; Nakajima, T.; Honda, Y.; Kitao, O.; Nakai, H.; Vreven, T.; Throssell, K.; Jr. Montgomery, J. A.; Peralta, J. E.; Ogliaro, F.; Bearpark, M. J.; Heyd, J. J.; Brothers, E. N.; Kudin, K. N.; Staroverov, V. N.; Keith, T. A.; Kobayashi, R.; Normand, J.; Raghavachari, K.; Rendell, A. P.; Burant, J. C.; Iyengar, S. S.; Tomasi, J.; Cossi, M.; Millam, J. M.; Klene, M.; Adamo, C.; Cammi, R.; Ochterski, J. W.

Martin, R. L.; Morokuma, K.; Farkas, O.; Foresman, J. B.; Fox, D. J. *Gaussian 09*; Gaussian Inc.: Wallingford, CT, 2016.

(63) Becke, A. D. Density functional exchange-energy approximation with correct asymptotic behaviour. *Phys. Rev. A: At., Mol., Opt. Phys.* **1988**, *38*, 3098–3100.

(64) Perdew, J. P. Density-functional approximation for the correlation energy of the inhomogeneous electron gas. *Phys. Rev. B: Condens. Matter Mater. Phys.* **1986**, *33*, 8822.

(65) Schaefer, A.; Huber, C.; Ahlrichs, R. Fully optimized contracted Gaussian basis sets of triple zeta valence quality for atoms Li to Kr. *J. Chem. Phys.* **1994**, *100*, 5829–5835.

(66) Marenich, A. V.; Cramer, C. J.; Truhlar, D. G. Universal solvation model based on solute electron density and on a continuum model of the solvent defined by the bulk dielectric constant and atomic surface tensions. *J. Phys. Chem. B* **2009**, *113*, 6378–6396.